J. Appl. Comput. Mech., xx(x) (2026) 1-13
DOI: 10.22055/jacm.2026.49355.5912

ISSN: 2383-4536
jacm.scu.ac.ir

Shahid Chamran
University of Ahvaz

Journal of
Applied and Computational Mechanics

Research Paper

# Analytical Solution of the Flow of Pseudo-plastic Fluid with the Effect of Inner Rotating Cylinder

Fozia Shaikh[1], Abdul Majeed Siddiqui[2], Ghulam Mustafa Memon[3], Syed Feroz Shah[1]

[1] Department of Basic Sciences & Related Studies, Mehran University of Engineering and Technology, Jamshoro, 76090, Pakistan,
Email: fozia.shaikh@faculty.muet.edu.pk (F.S.); feroz.shah@faculty.muet.edu.pk (S.F.S)

[2] Department of Mathematics, Pennsylvania State University, York Campus, York, PA 17403, USA, Email: ams5@psu.edu

[3] Interdisciplinary Research Center for Industrial Nuclear Energy, King Fahd University of Petroleum and Minerals,
Dhahran, 31261, Saudi Arabia, Email: ghulam.mustafa@kfupm.edu.sa

Received May 10 2026; Revised July 23 2026; Accepted for publication September 02 2026.
✉ Corresponding author: F. Shaikh (fozia.shaikh@faculty.muet.edu.pk)


**Abstract.** This study aims to develop an analytical solution for the circular Couette flow of shear-thinning fluid in the gap between coaxial cylinders, addressing the impact of the nonlinearity in the constitutive model. The Langlois Recursive Approach is applied to model the circular Couette flow of pseudoplastic fluids, offering a novel analytical framework that incorporates the effects of radius ratio, pseudo-plastic parameter, shear stress and friction factor ratio on flow dynamics. The findings have broad implications for practical applications, including journal bearings, mixing equipment, turbo machinery, viscometers, polymer processing, and drilling operations, where understanding the flow behavior of non-Newtonian fluids is critical. The analysis reveals that both the radius ratio and pseudo-plastic parameters significantly impact fluid velocity and shear stress. Additionally, a notable variation in pressure distribution is observed as centrifugal forces become dominant. Finally, to validate the obtained results, steady-state solutions for tangential motions are employed, successfully retrieving known solutions for Newtonian fluids documented in the literature.

**Keywords:** Non-Newtonian; Pseudo-plastic fluid; Steady; frictional factor; Langlois recursive.

## 1. Introduction

Taylor-Couette flow is a well-studied fluid flow phenomenon that occurs between two concentric cylinders, where one cylinder rotates while the other remains stationary. It is named after Couette and Taylor, who extensively studied this flow [1, 2]. This flow configuration has attracted significant research attention due to its potential to develop flow instabilities and its wide range of industrial applications. Such phenomena were investigated for viscous fluid experimentally by Couette. A circular Couette flow (CCF) is entirely azimuthal in its traditional form, where the inner cylinder rotates while the outer one remains stationary, maintaining a balance between the centrifugal force and the inward-pointing pressure gradient. This flow is relevant in cyclone separation and in the gap flow during fiber separation in the paper industry. Additionally, it finds applications in bearings and heat exchangers in the food industry. In his classical paper, Taylor presented the concept of viscous flow disturbance and noted that the rotation of cylinders is a key factor in the resulting circulating flow. Other factors, such as the radius ratio, gap size, and fluid properties, also play a significant role. The analysis of exclusively elastic Taylor-Couette instabilities, characterized by constant rotational velocity and first observed by Giesekus [3] in non-Newtonian fluids, revealed that elastic disturbances lead to significant nonlinear flow transformations. The stability of this flow has also been considered in several early experiments involving shear-thinning fluids also known as pseuo-plastic fluids having property that its viscosity decreases with respect to increase of shear rate. In some mechanized practices, such as oil-well cementing or greasing of spinning machinery, the fluids used are highly shear-thinning and slightly viscoelastic [4]. To isolate shear thinning impacts, non-Newtonian purely viscous fluids must be taken into account. For instance, there has been a noticeable rise in interest in comprehending fluids' hydrodynamic stability in many contexts, such as pipe flows, shear flows, or circulating flows, with a focus on very basic shear-thinning constitutive fluid models. Hüseyin Elçiçek, Bülent Güzel [5] experimentally studied the taylor-couette flow on the moving coaxial cylinders for power-law fluids. An experimental study on shear-thinning fluids in coaxial cylinders was conducted by Tatsuya Kawaguchi et al. [6]. Connecting with the shear thinning fluids, the rheological behavior of the complex fluids such as Williamson Nano fluid and casson Nano fluid on a porous boundary were investigated using similarity transformation [7, 8]. The rotating flow of Oldroyd-B fluid was investigated caused by the time-dependent pressure gradient employing a fractional operator [9]. Rotating systems like turbomachinery, grapheme oxide with water is effectual for thermal maintenance. Researchers have presented novel approaches for such type of geometries [10]. A piece of work was done using grapheme oxide nanoparticle numerically using MATLAB bvp4c solver to investigate the shape and behavior of nanoparticles in rotating geometry [11]. Numerical approaches, such as the shooting

Published online: September 04 2026

method and perturbation technique were used to solve the flow of a pseudo-plastic material between two rotating rolls by Aich, W et al. [12] which concluded that both methods yielded improved results. Alam et al. [13] examined the thin-film flow of an MHD pseudo-plastic fluid on a vertical wall.

In recent years, numerous studies have been conducted on flow structures in cylindrical geometries using non-Newtonian fluids. Remarkable research was conducted on thermal characteristics of Nano fluids and non-Newtonian fluid in the coaxial cylinders [14]. Authors have used numerical simulation for investigating the behavior of fluids and studied the various influential parameters thoroughly. Natural convected flow in the vertical annulus was numerically studied using finite volume method and SIMPLER algorithm in [15]. Researchers have beautifully explained the behavior of flow near inner and outer wall due to variation of the influential parameters and thermal effects. Megnetohydrodynamic convective flow of Nano fluids was examined in vertical porous cylinders numerically [16]. The analytical solution for Couette flow of a Giesekus fluid with an inner rotating cylinder was examined, presenting results for various mobility parameters that demonstrated the fluid's physical and mathematical behavior [17]. Homotopy perturbation method was applied to examine the flow in a concentric annulus where the outer cylinder is fixed and the inner cylinder rotates. The results indicated that the velocity was entirely dependent on the non-Newtonian parameter by Zeb et al. [18].

The Navier-Stokes equation can describe all existing fluids. For various rate-type fluids, non-linear mathematical models are established and analyzed using distinct approaches. These approaches have some limitations in its own. For perturbation, we required small parameter whereas homotopy polynomial is required for Homotopy perturbation method. Adomian decomposition method is suitable for nonlinear problems however when it comes to unsteady and strong nonlinearity, it fails to converges. On the other hand, numerical techniques are laborious and taking significant amount of time. Thus, reviewing the above literature it was concluded that the numerical and analytical description of flow becomes significantly more complicated in the case of fluids with non-linear constitutive equations [19]. In this paper, we thoroughly examined the significant potential of the novel approach known as 'Recursive Approach' for analyzing the flow of rate-type fluids. Notably, the study of rate-type special case of Oldroyd 8-constant fluid, known as, pseudo-plastic fluids is relatively underexplored area in the literature. Therefore, our research presents an advancement in the theoretical flow analysis of non-Newtonian rate-type pseudo-plastic fluids, particularly in the context of inner cylinder rotation. Langlois employed this approach, while neglecting the effects of inertia, to tackle problems requiring slow viscoelastic fluid flow only. Our study generalizes this approach to solve highly non-linear momentum equations with nonhomogeneous boundary conditions, representing a significant advancement. Moreover, since this method is conceptually and practically straightforward, it can be easily extended to higher orders. Following this approach, we will first employ the Langlois recursive method to obtain the velocity profile, stresses, and pressure profile for the tangential motion. The limiting case is also investigated by considering physical parameters, i.e., (pseudo-plastic parameter) $\beta \to 0$, (relaxation time) $\lambda_1 \to 0$, (material constant) $\mu_1 \to 0$, and solutions for the Newtonian fluid are discussed. This study provides insight into the behavior of fluid flow across cylinder gaps, particularly in relation to fluid mixing, painting and coating, lubrication systems, and polymerization processes, and helps to explain physical phenomena

## 2. Formulation of Mathematical Equations

We consider the flow of a pseudo-plastic liquid between two infinite coaxial cylinders. The outer cylinder has a fixed radius $R_0$ and remains stationary, while the inner cylinder has a radius $R_i (R_i < R_0)$ and rotates. We are assuming that inner cylinder is rotating with a constant angular velocity $\omega_i$. This arrangement signifies numerous engineering applications, including wire coating where wire is assumed as inner cylinder and melt polymer as fluid, journal bearings in which inner cylinder is shaft, lubricant as fluid, coaxial mixers containing inner rotating shaft and outer chamber, and similarly drilling fluid flow where drill pipe as inner cylinder, and mud as fluid. The dimensionless radius ratio $\xi = R_i / R_0$, $(0 < \xi < 1)$ characterizes the system, while the characteristic velocity is done by the inner cylinder, i.e., $\upsilon_i = (R_i \omega_i)$. In addition, the cylinders are assumed to be infinitely long, allowing us to neglect end effects and gravity is considered negligible compared to the shear forces caused by the rotation. In the case of circular Couette flow, we adopt cylindrical coordinates ($r$, $\theta$, $z$) to describe the motion of the fluid with $r$ spanning radially outward from the common centerline of the cylinders, and z aligns with this central axis. (See Fig. 1).

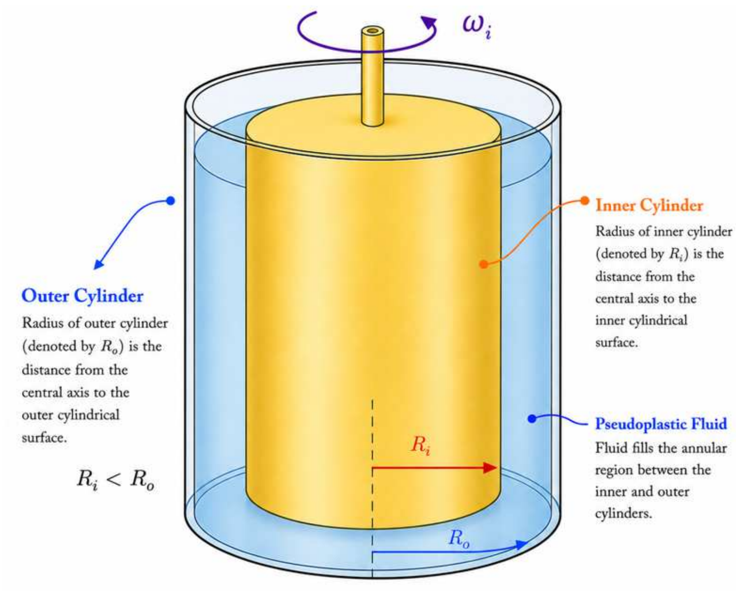


**Fig. 1.** Schematic geometry of inner rotating cylinder.

Since the fluid is assumed to be incompressible, its density remains constant. As a result, the fluid can only undergo isochoric motion, meaning its volume remains constant. Moreover, the flow is supposed to be steady $(\partial / \partial t = 0)$, so the continuity and momentum equation are explicitly given as [20]:

$$tr\dot{\gamma} = 0 \tag{1}$$

$$\rho\left[\left(\tilde{V}.\nabla\right)\tilde{V}\right] = \nabla .\tilde{T} + \rho g, \qquad \tilde{T} = -pI + \tilde{\varphi}. \tag{2}$$

Here $T$ is the Cauchy stress tensor, $-pI$ is the constitutively undetermined stress component caused by the incompressibility restriction, and $\rho$ is the constant density. $\varphi$ is the extra stress tensor and is different for different fluid models. Simple empirical models have been propositioned to portray the viscosity versus shear rate comportment of pseudo-plastic non-Newtonian fluids, thus in the present study, pseudo-plastic model has been adopted which was first introduced by Deiber [21] and having the similar properties presented in [22]:

$$\tilde{\varphi} + \lambda_1\left[\left(\tilde{V}.\nabla\right)\tilde{\varphi} - \left[L^t\tilde{\varphi} + \tilde{\varphi}L\right]\right] + \frac{\lambda_1 - \mu_1}{2}\left(\tilde{\dot{\gamma}}\tilde{\varphi} + \tilde{\varphi}\tilde{\dot{\gamma}}\right) = \eta\tilde{\dot{\gamma}}. \tag{3}$$

where $\dot{\gamma}(=L+L^t)$ is the rate of deformation and $L$ (= $gradV$), where $V$ is the velocity vector, $\eta$ is the zero-shear viscosity of the polymers, $\lambda_1$, the relaxation time and $\mu_1$ is the material constant. The time relaxation parameter influences the material's response to changing shear rates. In the limit $\lambda_1 = \mu_1$, one can retrieve the expression for the Maxwell fluid model, and in special cases, the Newtonian fluid model is achieved for $\lambda_1 \to 0$, $\mu_1 \to 0$.

Let $V_r$, $V_\theta$, and $V_z$ be the velocity of the fluid flow along the radial, circumferential, and axial directions respectively. Since the angular velocity is fixed, which is tempted by the rotation of the inner cylinder relative to the outer one, and the curvature of the surface is fixed, due to this, there is no flow of fluid along with radial and axial directions, i.e., $V_r = V_z = 0$. Though the flow is uniformly circumferential, hence velocity, stress, and pressure are the function of '$r$' only [5]. Thus:

$$\tilde{V} = (0, V_\theta(r)e_\theta, 0), \tilde{\varphi} = \tilde{\varphi}(r), p = p(r) \tag{4}$$

where $e_\theta$ is the unit vector in the θ-direction of the system of cylindrical coordinates.

To achieve a comprehensive understanding of the flow scenario under investigation, we introduce a set of dimensionless parameters. These parameters will facilitate a more insightful comparison with existing results documented in the literature. By employing the problem's geometric and boundary conditions, we proceed to non-dimensionalize the governing equations, thereby defining the relevant dimensionless groups that characterize the system [17]: $r^* = r / R_o, v^* = V_\theta / v_i, \lambda_1^* = \lambda_1 v_i / R_o, \mu_1^* = \mu_1 v_i / R_o$, $\beta^* = \beta / R_0, \varphi_{ij}^* = \varphi_{ij}\delta / \eta v_i, T^* = T\delta / \eta v_i, p^* = p\delta / \eta v_i,$ here $\delta = R_0(1-\xi)$ and is the radial distance of two cylinders. By introducing these conditions into governing equation (2) the dimensionless radial and tangential momentum equations take the form of:

$r$- component:

$$Re\left(-\frac{v^2}{r}\right) = -\frac{dp}{dr} + \frac{d\varphi_{rr}}{dr} + \frac{\varphi_{rr} - \varphi_{\theta\theta}}{r}. \tag{5}$$

$\theta$- component:

$$\frac{1}{r^2}\frac{d}{dr}(r^2\varphi_{\theta r}r) = 0. \tag{6}$$

where $\mathrm{Re} = \rho v_i R_0(1-\xi) / \eta = \rho v_i \delta / \eta$, being a rotational Reynolds number. It follows that:

$$(\tilde{V}.\nabla)\tilde{V} = \begin{bmatrix} \frac{-v^2}{r} & 0 \end{bmatrix}, \tag{7}$$

$$\tilde{\dot{\gamma}} = \begin{bmatrix} 0 & M \\ M & 0 \end{bmatrix}, \text{ where } M = r\frac{d}{dr}\left(\frac{v}{r}\right). \tag{8}$$

$$\tilde{\varphi} = \begin{bmatrix} 0 & -M\varphi_{rr} \\ -M\varphi_{rr} & -2M\varphi_{\theta r} \end{bmatrix}, \tag{9}$$

$$\left[\tilde{\dot{\gamma}}\tilde{\varphi} + \tilde{\varphi}\tilde{\dot{\gamma}}\right] = \begin{bmatrix} 2M\varphi_{\theta r} & M(\varphi_{rr} + \varphi_{\theta\theta}) \\ M(\varphi_{rr} + \varphi_{\theta\theta}) & 2M\varphi_{\theta r} \end{bmatrix}. \tag{10}$$

Taking assumption $(4)_1$ into account, the balance of mass equation (1) is satisfied identically and it is easy to prove that $\varphi_{zr} = \varphi_{rz} = \varphi_{z\theta} = \varphi_{\theta z} = \varphi_{zz}$ is zero whereas the dimensionless non-trivial components of extra stress tensor (3) are:

$$\varphi_{rr} + (\lambda_1 - \mu_1)M\varphi_{r\theta} = 0, \tag{11}$$

$$\varphi_{r\theta} - \frac{1}{2}(\lambda_1 - \mu_1)M\varphi_{rr} + \frac{1}{2}(\lambda_1 + \mu_1)M\varphi_{\theta\theta} = (1-\xi)M, \tag{12}$$

$$\varphi_{\theta\theta} - (\lambda_1 + \mu_1)M\varphi_{r\theta} = 0. \tag{13}$$

Making use of the above stress components, the nonlinear dimensionless Eqs. (5) and (6) for the considered geometry reads as:

$r$- momentum:

$$\frac{dp}{dr}=\frac{v^2}{r}-\frac{1}{Re}\left[\frac{(\lambda_1-\mu_1)}{r}\frac{d}{dr}\{r\mathrm{M}\varphi_{r\theta}\}-\frac{(\lambda_1+\mu_1)}{r}\mathrm{M}\varphi_{r\theta}\right]. \tag{14}$$

$\theta$- momentum:

$$\frac{1}{r^2}\frac{d}{dr}\left[r^2\left\{(1-\xi)\mathrm{M}+\frac{1}{2}(\lambda_1-\mu_1)\mathrm{M}\varphi_{rr}-\frac{1}{2}(\lambda_1+\mu_1)\mathrm{M}\varphi_{\theta\theta}\right\}\right]=0\ . \tag{15}$$

The boundaries of the annular region are essential for defining the geometry and conditions of the fluid flow. At the inner boundary, the fluid interacts with the inner cylinder, and the no-slip condition applies, meaning the fluid velocity matches the velocity of the inner cylinder. Since the outer cylinder does not move, the fluid velocity is zero at this boundary. In the polymer processes, the thicker polymers often stifle slip at the wall so current study consider the no-slip condition. Mathematically, these boundary conditions are expressed as follows [17]:

$$v(r)\big|_{r=\xi}=1,\quad v(r)\big|_{r=1}=0\quad \text{and}\quad p\big|_{r=1}=p_0\ . \tag{16}$$

## 3. Analytical Solutions for the Steady Flow

The Langlois Recursive Approach (LRA), suggested by Langlois [23], is a reliable method particularly suited for solving nonlinear equations that arise when non-Newtonian fluids are explored. Solving such nonlinear equations exactly is not an easy task. Following the Langlois Approach, the field variables [$v$, $p$, $T$, $\varphi$] appearing in the model Eqs. (14)-(15) are expanded into recursive series in the following form:

$$\tilde{v}=\sum_{n=1}^{\infty}\varepsilon^n v^{(n)}, \tag{17}$$

$$p=\text{constant}+\sum_{n=1}^{\infty}\varepsilon^n p^{(n)}, \tag{18}$$

$$\tilde{\varphi}=\sum_{n=1}^{\infty}\varepsilon^n \varphi^{(n)}, \tag{19}$$

$$\tilde{T}=\sum_{n=1}^{\infty}\varepsilon^n \mathrm{T}^{(n)}. \tag{20}$$

where $\varepsilon$ is a small dimensionless number. By the recursive expansions Eqs. (17)-(20) switched into the simplified governing equations and boundary conditions precede to a series of hierarchically linearized balancing equations $\left[v^{(n)},\ p^{(n)},\ T^{(n)}\right]$, $n=1,2,3,$ to be solved successively. Subsequently, the solution $\left[v^{(1)},\ p^{(1)},\ T^{(1)}\right]$ agrees well with the governing equation for the linear viscous flow associated with the non-homogeneous boundary conditions. The set of equations of second order related to $\left[v^{(2)},\ p^{(2)},\ T^{(2)}\right]$ is comparable except for the non-homogeneous part containing the statements for $\left[v^{(1)},\ p^{(1)},\ T^{(1)}\right]$ with homogenous boundary conditions. The equations of the third order corresponding to $\left[v^{(3)},\ p^{(3)},\ T^{(3)}\right]$ are also comparable excluding the non-homogenous part comprising in the term of $\left[v^{(1)},\ p^{(1)},\ T^{(1)},\ v^{(2)},\ p^{(2)},\ T^{(2)}\right]$ with homogenous boundary conditions; henceforth, the contribution of the pseudo-plastic term is provided in the third order equations.

For including new contributions resulting from the cylindrical-shaped geometry, calculations up to $O(\varepsilon^3)$ are adequate. However, if more data is required, it is simple to further extend the analysis to higher-order terms.

### 3.1. First order problem and solution O($\varepsilon$): Newtonian flow

Following the recursive approach (17)-(20) and solution procedure framed in Section 3, the linearized mass conservation and momentum balance equations emanating at each order of Eqs. (14)-(15) and Eq. (16), we achieve:

$$\frac{dv^{(1)}}{d\theta}=0, \tag{21}$$

$$\frac{d\mathrm{P}^{(1)}}{dr}=0, \tag{22}$$

$$\frac{d}{dr}\left\{r^2(1-\xi)\left(\frac{dv^{(1)}}{dr}-\frac{v^{(1)}}{r}\right)\right\}=0, \tag{23}$$

$$\mathrm{T}_{r\theta}{}^{(1)}=(1-\xi)r\frac{d}{dr}\left(\frac{v^{(1)}}{r}\right),\qquad \mathrm{T}_{rr}{}^{(1)}=-p^{(1)}+\varphi_{rr}{}^{(1)},\quad \mathrm{T}_{\theta\theta}{}^{(1)}=-p^{(1)}+\varphi_{\theta\theta}{}^{(1)}. \tag{24}$$

The boundary conditions associated with the equations of first order are given as:

$$v^{(1)}(r)\big|_{r=\xi}=1,\ \ v^{(1)}(r)\big|_{r=1}=0,\quad p^{(1)}(r)\big|_{r=1}=p_0. \tag{25}$$

The incompressibility Eq. (21) is satisfied identically and the integration of Eqs. (22) and (23) with the non-homogenous boundary conditions (25) produces the following well-known formula [5]:

$$v^{(1)}=Ar+\frac{B}{r}. \tag{26}$$

with,

$$p^{(1)}=\text{constant}. \tag{27}$$

where $A$ and $B$ appearing in Eq. (26) are expressed in order to impose the no slip conditions at inner wall:

$$A=-\frac{\xi}{1-\xi^2}\quad \text{and}\quad B=\frac{\xi}{1-\xi^2}. \tag{28}$$

At $O(\varepsilon)$ the extra stress components (24), invoking Eq. (26), yields:

$$T_{rr}{}^{(1)}=-p_0=T_{\theta\theta}{}^{(1)},\ \ T_{r\theta}{}^{(1)}=-\frac{2\xi}{1+\xi}\frac{1}{r^2}. \tag{29}$$

By structure, the solution complies fully with the well-known Newtonian solution at the leading first order with no pseudo-plastic effects [5, 24, 25].

### 3.2. Second order problem and solution $O(\varepsilon^2)$

The boundary value system produced by second-order linearization is as follows:

$$\frac{dv^{(2)}}{d\theta}=0, \tag{30}$$

$$\frac{dP^{(2)}}{dr}=\frac{v^{(1)2}}{r}-\frac{1}{\text{Re}}\frac{(\lambda_1-\mu_1)(1-\xi)}{r}\frac{d}{dr}\left\{r\left(\frac{dv^{(1)}}{dr}-\frac{v^{(1)}}{r}\right)\right\}^2-\frac{1}{\text{Re}}\frac{(\lambda_1-\mu_1)(1-\xi)}{r}\left(\frac{dv^{(1)}}{dr}-\frac{v^{(1)}}{r}\right)^2, \tag{31}$$

$$\frac{1}{r^2}\frac{d}{dr}\left\{r^2(1-\xi)\left(\frac{dv^{(2)}}{dr}-\frac{v^{(2)}}{r}\right)\right\}=0. \tag{32}$$

The elements of tensor in this order $O(\varepsilon^2)$, introducing the first and second order velocity [$v^{(1)}$, $v^{(2)}$] are then obtained as:

$$T_{rr}{}^{(2)}=-p^{(2)}-(\lambda_1-\mu_1)(1-\xi)\left(\frac{dv^{(1)}}{dr}-\frac{v^{(1)}}{r}\right)^2, \tag{33}$$

$$T_{r\theta}{}^{(2)}=(1-\xi)\left(\frac{dv^{(2)}}{dr}-\frac{v^{(2)}}{r}\right), \tag{34}$$

$$T_{\theta\theta}{}^{(2)}=-p^{(2)}+(\lambda_1+\mu_1)(1-\xi)\left(\frac{dv^{(1)}}{dr}-\frac{v^{(1)}}{r}\right)^2. \tag{35}$$

The second order correction satisfy:

$$v^{(2)}(r)\big|_{r=\xi,\,1}=0,\quad p^{(2)}(r)\big|_{r=1}=0. \tag{36}$$

The second-order linear differential equation (32) is mechanically analogous to Eq. (23) aside from the non-homogeneous component. Having a solution to the first-order equations, it is easy to show the second-order solution by integrating Eqs. (31) and (32):

$$v^{(2)}=0, \tag{37}$$

$$p^{(2)}=\left[\frac{A^2}{2}(r^2-1)+2AB\ln(r)-\frac{B^2}{2}\left(\frac{1}{r^2}-1\right)\right]-\frac{2(\lambda_1-2\mu_1)(1-\xi)}{\text{Re}}\left(\frac{1}{r^4}-1\right)B^2, \tag{38}$$

With the physical stresses defined by Eqs. (33)-(35) takes the form:

$$T_{rr}{}^{(2)}=-\frac{A^2}{2}(r^2-1)+2AB\ln(r)-\frac{B^2}{2}\left(\frac{1}{r^2}-1\right)+\frac{2(\lambda_1-2\mu_1)(1-\xi)}{\text{Re}}\left(\frac{1}{r^4}-1\right)B^2-\frac{(\lambda_1-\mu_1)(1-\xi)}{r^4}B^2, \tag{39}$$

$$T_{r\theta}{}^{(2)}=0, \tag{40}$$

$$T_{\theta\theta}{}^{(2)} = -\frac{A^2}{2}\left(r^2-1\right) + 2AB\ln(r) - \frac{B^2}{2}\left(\frac{1}{r^2}-1\right) + \frac{2(\lambda_1-2\mu_1)(1-\xi)}{\mathrm{Re}}\left(\frac{1}{r^4}-1\right)B^2 + \frac{(\lambda_1+\mu_1)(1-\xi)}{r^4}B^2. \tag{41}$$

Here the $A=-\xi/(1-\xi^2)$, $B=\xi/(1-\xi^2)$, and $\beta=(\lambda_1^2-\mu_1^2)$. Since there isn't a source-like term in Eq. (32) it must meet the no-slip homogeneous boundary condition and consequently evanescence at the cylinder boundaries. Moreover, it is worth noting that the pressure field for the inner rotating cylinder for $\beta \to 0$ fully agrees with the classical results [26].

### 3.3. Third order and solution at O($\varepsilon^3$), pseudo-plastic fluid

The third order set of boundary value problem in terms of the first and second order velocity using the recursive assumptions (17)-(20) are computed and collected as:

$$\frac{dv^{(3)}}{d\theta} = 0, \tag{42}$$

$$\frac{dP^{(3)}}{dr} = 2\frac{v^{(1)}v^{(2)}}{r} - \frac{2(\lambda_1-\mu_1)(1-\xi)}{r\,\mathrm{Re}}\frac{d}{dr}\left\{r\left(\frac{dv^{(1)}}{dr}-\frac{v^{(1)}}{r}\right)\left(\frac{dv^{(2)}}{dr}-\frac{v^{(2)}}{r}\right)\right\} - \frac{2(\lambda_1+\mu_1)(1-\xi)}{r\,\mathrm{Re}}\left(\frac{dv^{(1)}}{dr}-\frac{v^{(1)}}{r}\right)\left(\frac{dv^{(2)}}{dr}-\frac{v^{(2)}}{r}\right), \tag{43}$$

$$\frac{1}{r^2}\frac{d}{dr}\left\{r^2(1-\xi)\left(\frac{dv^{(3)}}{dr}-\frac{v^{(3)}}{r}\right) - \beta r^2(1-\xi)\left(\frac{dv^{(1)}}{dr}-\frac{v^{(1)}}{r}\right)^3\right\} = 0, \tag{44}$$

$$T_{rr}{}^{(3)} = -p^{(3)} - 2(\lambda_1-\mu_1)(1-\xi)\left(\frac{dv^{(1)}}{dr}-\frac{v^{(1)}}{r}\right)\left(\frac{dv^{(2)}}{dr}-\frac{v^{(2)}}{r}\right), \tag{45}$$

$$T_{r\theta}{}^{(3)} = (1-\xi)\left(\frac{dv^{(3)}}{dr}-\frac{v^{(3)}}{r}\right) - \beta(1-\xi)\left(\frac{dv^{(1)}}{dr}-\frac{v^{(1)}}{r}\right)^3, \tag{46}$$

$$T_{\theta\theta}{}^{(3)} = -p^{(3)} + 2(\lambda_1+\mu_1)(1-\xi)\left(\frac{dv^{(1)}}{dr}-\frac{v^{(1)}}{r}\right)\left(\frac{dv^{(2)}}{dr}-\frac{v^{(2)}}{r}\right). \tag{47}$$

Related transformed homogenous boundary conditions:

$$v^{(3)}(r)\Big|_{r=\xi,1} = 0, \quad p^{(3)}(r)\Big|_{r=1} = 0. \tag{48}$$

At O($\varepsilon^3$), Eq. (42) is identically satisfied, and seeking the solution for velocity and pressure field using first and second-order solutions, we arrive at:

$$v^{(3)} = -\frac{4\beta}{3\xi(1-\xi^2)^3}\left[\frac{\xi^4}{r^5} - \frac{\left(\xi^4+\xi^2+1\right)}{r} + \left(\xi^2+1\right)r\right], \tag{49}$$

$$p^{(3)} = 0. \tag{50}$$

In a similar way, the third order stress components rendering from Eqs. (45)-(47) using Eq. (49):

$$T_{rr}{}^{(3)} = 0 = T_{\theta\theta}{}^{(3)}, T_{r\theta}{}^{(3)} = \frac{8\beta(1-\xi)}{3\xi\left(1-\xi^2\right)^3}\left[\frac{\xi^4+\xi^2+1}{r^2}\right]. \tag{51}$$

In contrast with O($\varepsilon^2$), contribution of pseudo-plastic parameter emerged to the torsional flow in the leading order O($\varepsilon^3$). In this fashion, all the results for the pseudo-plastic fluid flow are computed up to O($\varepsilon^3$) are then encapsulated as:

$$V = \frac{\xi}{1-\xi^2}\left[\frac{1}{r}-r\right] - \frac{4\beta}{3\xi(1-\xi^2)^3}\left[\frac{\xi^4}{r^5} - \frac{\left(\xi^4+\xi^2+1\right)}{r} + \left(\xi^2+1\right)r\right], \tag{52}$$

$$p - p_0 = \frac{Re\,\xi^2}{\left(1-\xi^2\right)^2}\left[\frac{r^2-1}{2} + 2\ln(r) - \frac{1}{2}\left(\frac{1}{r^2}-1\right)\right] - 2\beta\frac{\xi^2(1-\xi)}{\left(1-\xi^2\right)^2}\left(\frac{1}{r^4}-1\right), \tag{53}$$

$$T_{rr} = p_0 - \frac{\xi^2}{\left(1-\xi^2\right)^2}\left[\frac{r^2-1}{2} + 2\ln(r) - \frac{1}{2}\left(\frac{1}{r^2}-1\right) - \frac{2(\lambda_1-2\mu_1)(1-\xi)}{Re}\left(\frac{1}{r^4}-1\right) - \frac{4(\lambda_1-\mu_1)(1-\xi)}{r^4}\right], \tag{54}$$

$$T_{\theta\theta} = p_0 - \frac{\xi^2}{\left(1-\xi^2\right)^2}\left[\frac{r^2-1}{2} + 2\ln(r) - \frac{1}{2}\left(\frac{1}{r^2}-1\right) - \frac{2(\lambda_1-2\mu_1)(1-\xi)}{Re}\left(\frac{1}{r^4}-1\right) + \frac{4(\lambda_1+\mu_1)(1-\xi)}{r^4}\right], \tag{55}$$

$$T_{r\theta} = -\frac{2\xi}{1-\xi^2}\frac{1}{r^2} + \frac{8\beta(1-\xi)}{3\xi\left(1-\xi^2\right)^3}\left[\frac{\xi^4+\xi^2+1}{r^2}\right]. \tag{56}$$

It is apparent from the results that for $\beta \to 0$, the result for the velocity and shear stress is the same as the typical classical Newtonian fluid. Moreover, the first term on right side of Eq. (53) defines the centrifugal force which rises from the rotational motion of the cylinder and generates the pressure from inner to outer. This term is always positive due to centrifugal force and pressure increases from inner to outer. The second term arise from the normal stress components which are inherent to pseudoplastic fluids due to their viscoelastic nature. On the other hand, to balance the effect of centrifugal force and normal stresses, radial pressure gradient has been computed by differentiating Eq. (53) is given below as:

$$\frac{dp}{dr} = \frac{Re\,\xi^2}{\left(1-\xi^2\right)^2}\left[r + \frac{2}{r} + \frac{1}{r^3}\right] + 8\beta\frac{\xi^2(1-\xi)}{\left(1-\xi^2\right)^2}\left(\frac{1}{r^5}\right). \tag{57}$$

Equations (53) and (57) represent the excellent agreement with the classical results of Newtonian fluid if $\beta \to 0$ and the results are similar to the dimensional form of the result presented in [26, 27].

## 4. Friction Factor

In procedural applications involving the studied phenomenon, a crucial parameter that needs to be determined is the torque per unit length entailed to rotate the internal cylinder [27]:

$$\Im = (-T_w)\xi(2\pi\xi L). \tag{58}$$

In the viscometer, the force is transmitted to the fluid when the inner cylinder instigates rotation about its axis causing the fluid to deform and then travel to the outer cylinder. As a consequence, the force exposed on the inward wall pointing momentum flux $(T_w = T_{r\theta}|_{r=\xi})$ at the surface of the cylinder and reads as:

$$T_w = T_{r\theta}\big|_{r=\xi} = -\frac{2}{\xi(1+\xi)} + \frac{8\beta(1-\xi)}{3\left(1-\xi^2\right)^3}\left[\frac{\xi^4+\xi^2+1}{\xi^3}\right]. \tag{59}$$

In Couette flow, the friction factor term plays a significant role in understanding the dynamics of the flow. It helps quantify how the velocity of the fluid varies across the annular gap between the rotating inner cylinder and the stationary outer cylinder. The friction factor ($f$) is a dimensionless quantity that characterizes the amount of wall shear stress, or resistance to shear, within a fluid flow and can be described as:

$$f = 2\left|\frac{T_{r\theta}|_{r=\xi}}{\rho v_i^2}\right|. \tag{60}$$

It can be noticed from Eq. (60) that the friction factor, $f$, depends primarily on the velocity $v_i$, radius ratio $\xi$, and density $\rho$. In the customary, we calculate the product of friction factor and rotational Reynolds number as $f\mathrm{Re} = -2T_w$. If the values of torque for pseudo-plastic fluid $\Im$ are normalized with the corresponding Newtonian fluid $\Im_N$, we gained the following correlation [25]:

$$\frac{\Im}{\Im_N} = \frac{f\,\mathrm{Re}}{(f\,\mathrm{Re})_N} = -\frac{\xi(1+\xi)}{2}T_w. \tag{61}$$

which shows that the impact of the $\beta$ and $\xi$ on torque is similar to the $f$Re. The limiting value of the tangential shear stress at the internal cylinder $T_w$, as $\beta \to 0$, i.e., $T_w = -2/\xi(\xi + 1)$. This expression, which is a function exclusively of the radius ratio $\xi$, represents the well-established wall shear stress for Newtonian fluids, characterized by the absence of shear-thinning effects. The solution (61) in our work is similar to the Eq. (34) in [17].

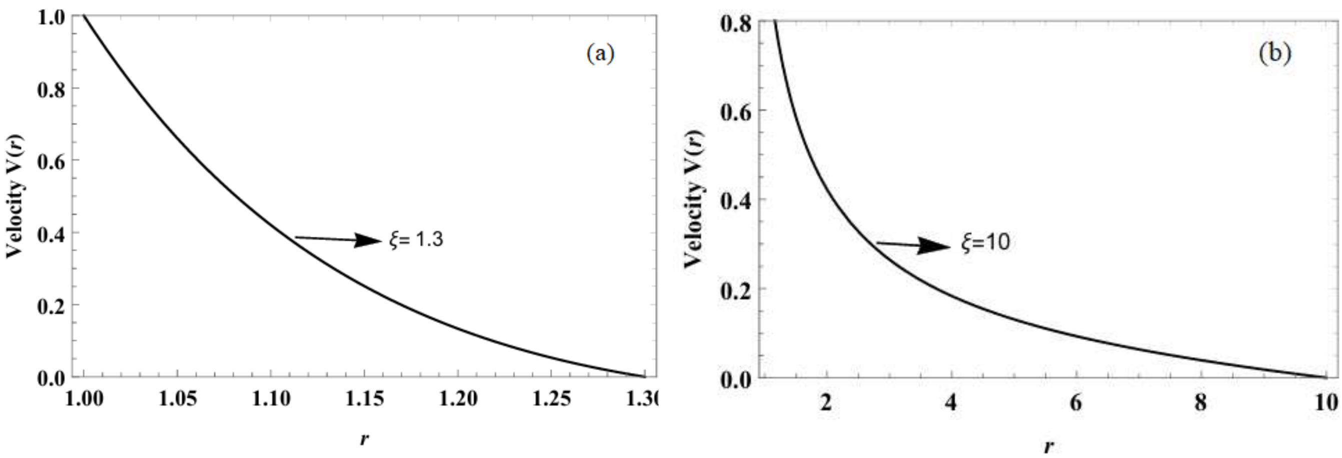


**Fig. 2.** Effect of radius ratio on dimensionless Tangential Velocity V(r) for fixed $\beta$ = 0.1.

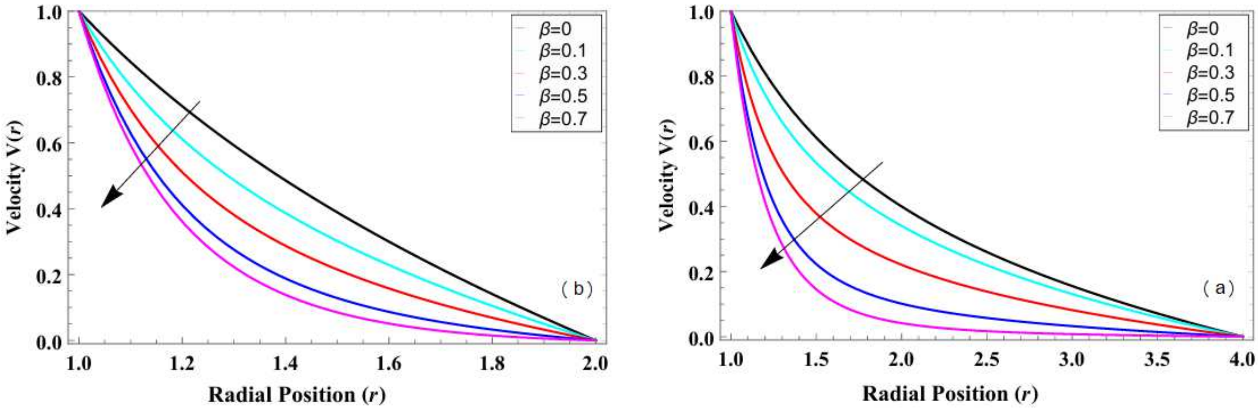


**Fig. 3.** Effect of Pseudo-plastic parameter on dimensionless Tangential Velocity V(r) when (a) $\xi$ = 0.5; (b) $\xi$ = 0.1.

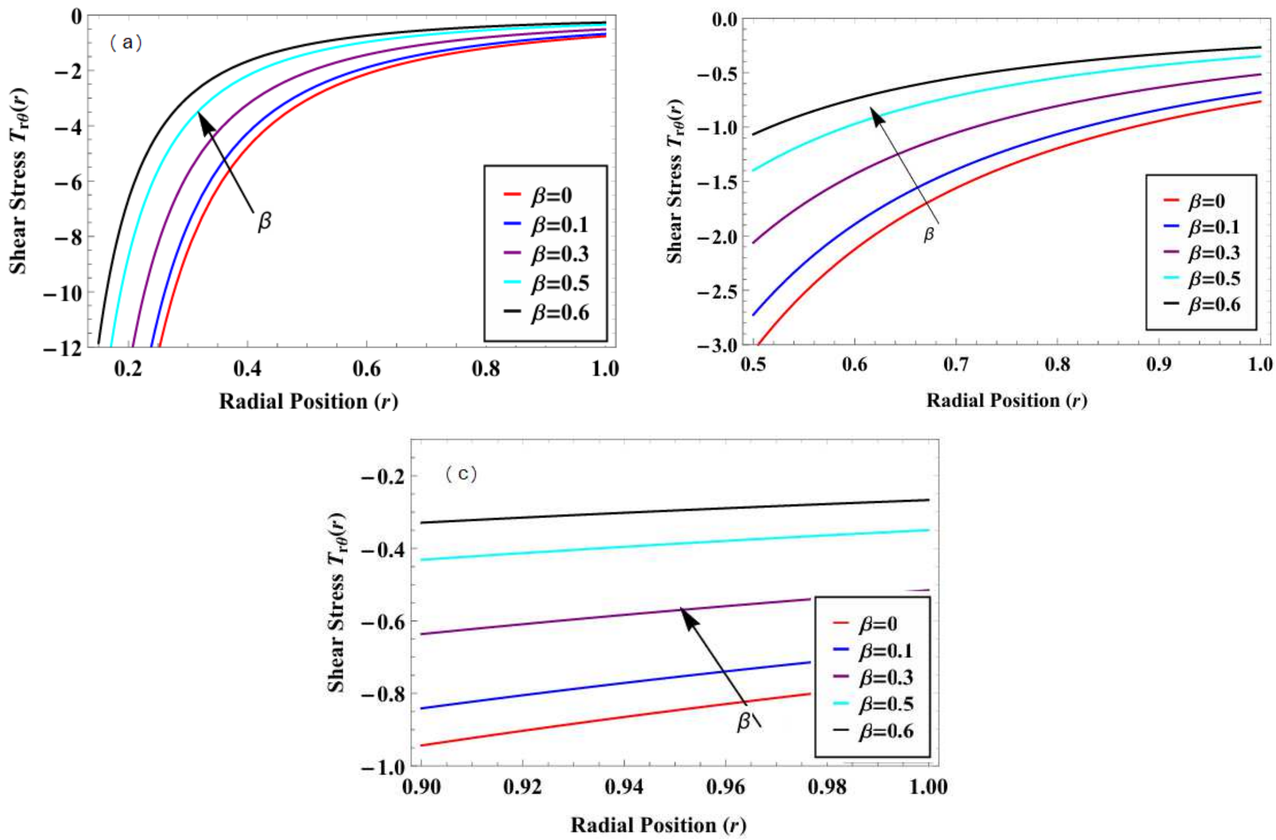


**Fig. 4.** Effect of Pseudo-plastic parameter on dimensionless Shear stress $T_{r\theta}(r)$ when (a) $\xi$ = 0.1; (b) $\xi$ = 0.5; (c) $\xi$ = 0.9.

## 5. Results and Discussion

This section discusses the findings pertaining to the Pseudo-plastic non-Newtonian fluid flow between coaxial cylinders where inner cylinder rotated and the outer cylinder remained fixed. The key parameters investigated include velocity profiles, shear stress distribution, pressure profile and friction factor. Furthermore, with the focus on portraying a comprehensive vision of how the pseudo-plastic fluid behaves in the cylinders, the results rendered below are investigated using the analytical approach and contrasted with a range of feasible values to predict the physical behavior of the shear thinning fluid for the radius ratio $\xi$ (= 0.1; 0.5; 0.9; 1.3; 2; 4; 10;), Reynolds number Re (= 1; 10; 100;), and pseudo-plastic parameter $\beta$ (= 0; 0.1; 0.3; 0.5; 0.6; 0.7) using Mathematica 11.9. Our results are validated by fabricating a contrast with theoretical predictions and previous studies in a limiting sense.

As anticipated, the velocity solution in Eq. (52) aligns with the classic circular Couette flow. However, Figs. 2(a) and 2(b) vividly illustrate the intriguing effects of varying the fluid's radius ratio, with the pseudo-plastic parameter fixed at $\beta$ = 0.1, offering insights from both mathematical and physical perspectives. In Fig. 2(a), the velocity profiles for a radius ratio $\xi$ = 1.3 reveal a pronounced peak near the inner cylinder, gradually tapering off towards the outer cylinder. In addition, the profile grows straight and linear. Conversely, Fig. 2(b), which depicts a radius ratio of $\xi$ = 10, shows a similarly peaked velocity profile, but with a fascinating twist: the flow arrangement near the inner cylinder exhibits a noticeable variation. The velocity profile here is not only maximal but also extends more uniformly across the radial direction, reflecting the increased influence of the inner cylinder's rotation. This flow behavior within the gap exhibits similarities to the flow between parallel plates.

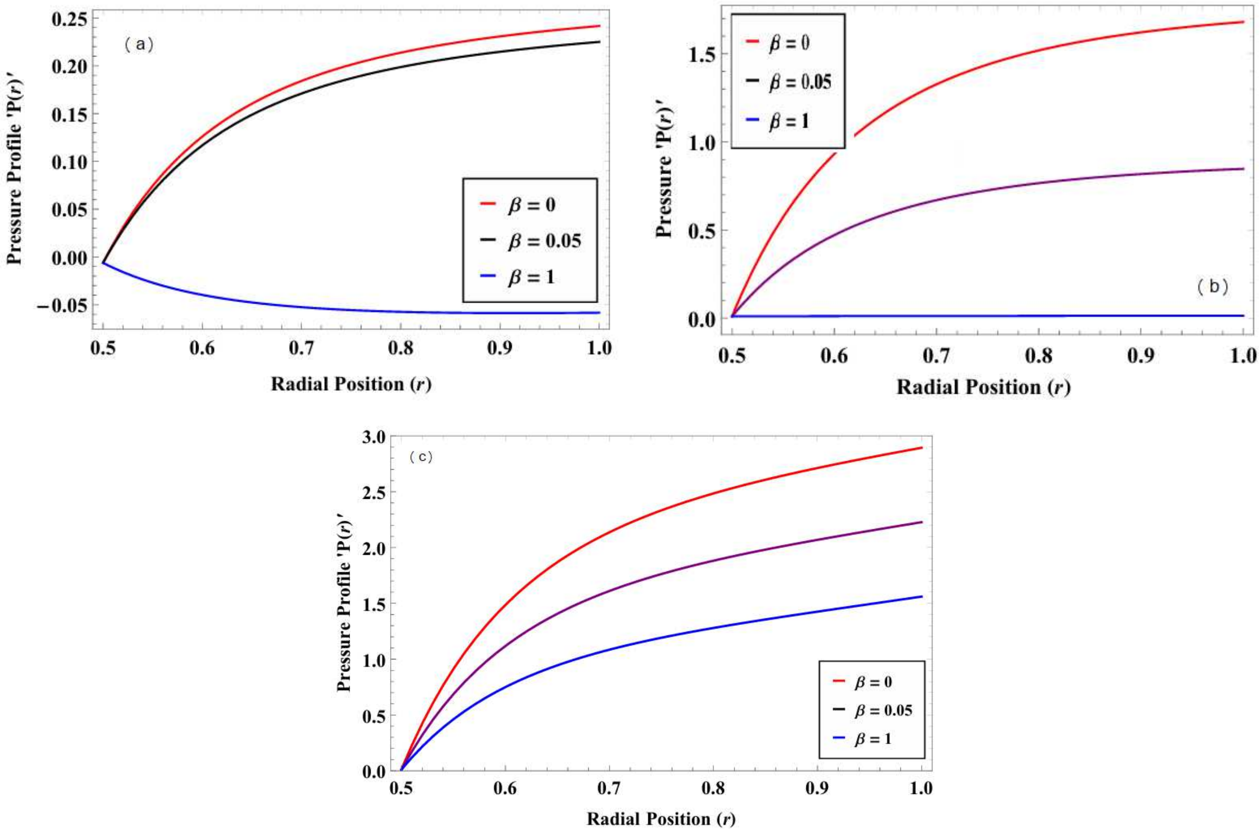


**Fig. 5.** Effect of Reynolds number on dimensionless Pressure profile $p(r)$ when (a) $\xi$ = 0.1, Re = 1; (b) $\xi$ = 0.5, Re = 10; (c) $\xi$ = 0.9, Re = 50.

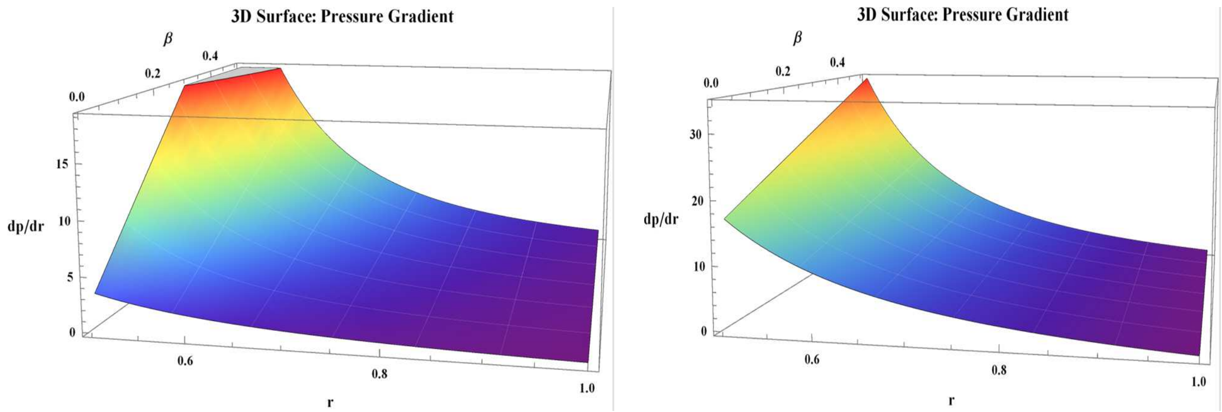


**Fig. 6.** Effect of Reynolds number on dimensionless Pressure Gradient $dp/dr$ when (a) $\xi$ = 0.5, Re = 1; (b) $\xi$ = 0.5, Re = 10.

Concerning the influence of pseudo-plastic parameters on tangential velocity, Figs. 3(a) and 3(b) present velocity profiles for radius ratios $\xi$ = 0.5 and $\xi$ = 0.1, comparing a Newtonian fluid to the selected values of the pseudo-plastic parameter $\beta$. For $\beta$ = 0, the dimensionless velocity distribution mirrors that of a Newtonian fluid, demonstrating an identical profile. However, the couple effect of pseudo-plastic parameter $\beta$ and rotation of inner cylinder indicates a pronounced shift in velocity. The dimensionless velocity near the inner cylinder is pronounced, while a corresponding reduction is observed near the outer cylinder for both radius ratios by the enhanced motion of the inner cylinder. Physically, as β rises, the shear-thinning behavior decreases, the relaxation time of fluid particles extends, leading to a more pronounced impact of viscosity on the flow regime. This heightened viscosity introduces additional resistance to the movement of fluid particles, causing the velocity profile to exhibit a marked decline. Moreover, Eq. (52) demonstrates that our findings are the same as the results of Ravanchi [25], and Dapra [17] as it is $\beta$ = 0 (i.e., by fixing We = 0 and De = 0 in Eqs. (28) and (31) of their works). Moreover, increasing the shear thinning effect for various values of non-Newtonian pseudo-plastic parameter $\beta$ = 0.1 to 0.6 fixing $\xi$ = 0.5 is also analogous to the literature [24] (i.e., with decreasing $n$ in their work).

The influence of the material property on dimensionless shear stress is shown in Fig. 4(a), 4(b), and 4(c) plotted against radial distance for different radius ratio $\xi$ and the same pseudo-plastic parameter $\beta$ mentioned above, illustrating the behavior of shear-thinning of the pseudo-plastic model. Fig. 4(a) (with $\xi$ = 0.1), demonstrates that rising radial distance $r$, the absolute value of $T_{r\theta}$ decreasing along with its gradient; comparable patterns are seen in Figs. 4(b) and 4(c). This impact intensifies for $\xi$ = 0.1 (Fig. 4(a)) and weakens for $\xi$ = 0.9 (Fig. 4(c)), as the dimensionless shear stress remains relatively constant, similar to that observed in planar Couette flow. It can be noteworthy that a rise in the pseudo-plastic parameter induces an in higher strain rate of the fluid near the rotating inner cylinder, which eventually slackens its shear viscosity and confirms the shear-thinning behavior.

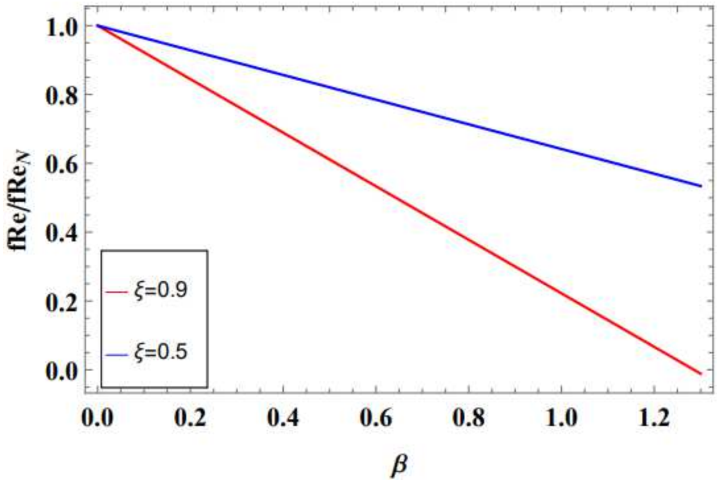


**Fig. 7.** Effect of radius ratio on Normalized Frictional factor versus pseudo-plastic parameter.

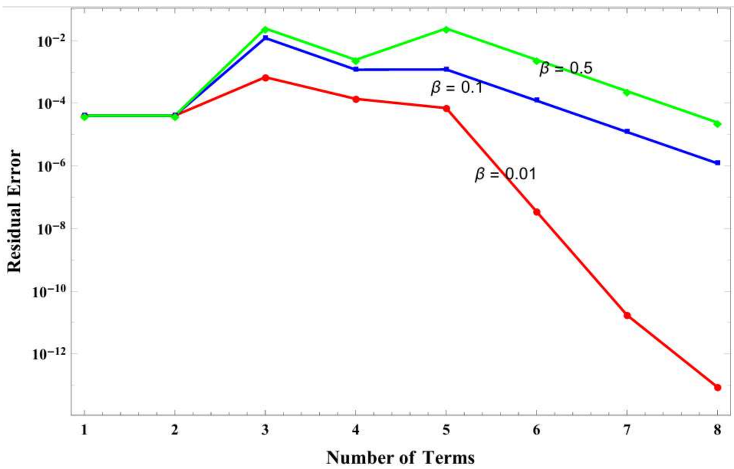


**Fig. 8.** Residual error verses Order terms for different $\beta$.

The pressure change is defined in Eq. (53) as the fluid moves radially away from the axis of rotation (from the inner to the outer cylinder). This movement essentially drives the fluid radially outward. In Couette flow, the pressure typically decreases toward the inner cylinder as the fluid moves radially outward due to the centrifugal force generated by the rotation of the inner cylinder. Figures 5(a) to 5(c) depict pressure fluctuations concerning psudo-plastic properties and centrifugal force. Figure 5(a) portrays the relative effects of the fluid psudo-plastic property on the pressure profile within the annulus space where the centrifugal force is minimal (i.e., Re = 1). For Newtonian fluids, the difference between first and second normal stress is negligible in shear flow, and pressure rises with the surge of radius ($dp/dr = \rho v^2/r > 0$). For shear-thinning fluids, the first normal stress difference is reasonably negative and has a significantly greater absolute value than the second normal stress difference. In this instance, pressure drops radially as shown in Fig. 5(a). However, the pressure gradient in this case increases with $\beta$ which confirms the pseudo-plasticity of the fluid that intensifies the pressure gradient. This trend can be seen in the 3D surface plot in Fig. 6(a).

The impact of centrifugal force on the pressure for Reynolds number (e.g., Re = 10) is shown in Fig. 5(b) whereas impact of (Re = 10) on pressure gradient can be seen in Fig. 6(b). Figure 5(b) shows that the pressure increases in radial direction while decreases with an increasing the pseudo-plastic parameter. The motion of the inner cylinder exerts centrifugal forces that significantly influence the structure of the resulting flows. Since the velocity at inner cylinder is enhanced due to the shear thinning behavior of the fluid, consequently, increases centrifugal force. A dominant centrifugal force needs a higher pressure-gradient to make it stable, however, as the fluid moves radially, pressure gradient decreases that also satisfy the $dp/dr = \rho v^2/r$ *where pressure gradient is inversely proportional to radial component*. This trend is clear highlighted in Fig. 6(b) which validates the physical behavior of shear thinning fluids in rotating coaxial cylinders. Figure 5(c) depicts the varying pattern of pressure in the annular space under condition of predominant centrifugal force (i.e., Re = 50). Comparatively, in the case of a pseudo-plastic fluid, at higher Reynolds numbers, centrifugal force becomes dominate. With the shorter pseudo-plastic parameter, the effective viscosity decreases, leading to shear thinning behavior. Additionally, it was found that enhancing the material characteristics reduces pressure variation across the annulus because the velocity decreases throughout the annulus.

Figure 7 illustrates the motion of the inner cylinder and the effect of the fluid material property on $f$Re, which is normalized with the associated Newtonian value ($f\mathrm{Re}_N = 4/\xi(1+\xi)$). The apparent viscosity reduces as the pseudo-plastic parameter $\beta$ increases, while the flow rate rises with $\beta$. The Shear-thinning behavior of the fluid is evident from Fig. 6, where the averaged friction factor at the inner wall is plotted. Thus, higher pseudo-plasticity reduces the rotational torque of the cylinder (as indicated by the friction factor). Clearly, the shear rate-dependent viscosity is more pronounced in the rotating inner cylinder, where the thickness of the boundary layer diminishes with rising $\beta$. Since viscosity measures a fluid's resistance to flow or change in form, lower viscosity results in reduced friction. The similar trend has been noticed in [25].

## 6. Validation of the Langlois Recursive Approach

The Langlois Recursive Approach (LRA) is validated through its inherent theoretical consistency as presented in section 5. The series exactly recovers the classical Newtonian fluid for $\beta = 0$ that upholds the accuracy and sturdiness of the recursive approach (see Eqs. (52)-(59)). In addition, the convergence of the Langlois Recursive Method is proven through inclusive residual analysis, which describes that the residual error diminishes as the number of terms increases. The residual $R(r)$ is calculated by introducing the approximate solutions into the governing nonlinear equations. For the third order solution, the residual is:

$$R(r) = -\frac{32\beta\xi^3}{\left(1-\xi^2\right)^3 r^7} + O\left(\beta^2\right). \tag{62}$$

It is apparent that the residual is proportional to $\beta$, ratifying converges to the classical Newtonian solution when the $\beta \to 0$. The maximum residual declines rapidly as $r^{-7}$. The convergence of the LRA is governed by the condition below:

$$|\beta| < \beta_{max} = \frac{\xi^2\left(1-\xi^2\right)^2}{4}. \tag{63}$$

As a validation test, Fig. 8 demonstrates the residual error verses number of terms for different pseudo-plastic parameter $\beta$ fixing $\xi = 0.5$ (moderate gap). For the small value of $\beta$, the first and second terms are same because of $\upsilon^{(2)} = 0$. Since the third term is the implementation of the pseudo-plastic behaviour, residual error slightly jumps and drops steadily as the number of terms increases. This represents the stable convergence of the approach for coaxial cylinders. Moreover, with increasing the values of pseudo-plastic parameter $\beta$, the small jump is seen at term 3, however, the maximum residual error for this value is $10^{-2,}$ it still converges as the number of terms increases, however, error reduces. Furthermore, for $\beta = 0.5$, oscillations are seen, however, overall reduction of the error occurs. Thus, the residual analysis affirms the stability and convergence of the Langlois Recursive Approach within the defined parameters.

## 7. Conclusion

The Langlois recursive approach has demonstrated remarkable effectiveness in addressing highly non-linear ordinary differential equations (ODEs) and partial differential equations (PDEs). This study successfully applied the Langlois Recursive Approach (LRA) to obtain an approximate analytical solution for the rotating flow of pseudoplastic fluid in coaxial cylinders. The derived analytical expressions for velocity components, pressure distribution, shear stress, and frictional factor in dimensionless form were thoroughly analyzed across various values of radius ratio, Reynolds numbers, and pseudo-plastic parameters. The predicted values for assorted flow parameters show the physical exemplification of the shear-thinning behavior of fluid stimulated by a rotating cylinder.

The obtained results show the following findings:

- By increasing the pseudo-plastic parameter, the velocity distribution decreases since an enhancement in viscosity is introduced.
- In the case of small radius ratios, the velocity profile follows a linear pattern.
- The decreasing effect of shear stress is observed for the various values of pseudo-plastic parameters.
- As compared to Newtonian fluids, pseudo-plastic fluids have weaker pressures.
- Increasing the Reynolds number leads to more centrifugal force while reducing the Reynolds number leads to less centrifugal force.
- Comparatively, for a higher Reynolds number, pressure increases whereas decreases with increasing relaxation time.
- A rise in the fluid material properties causes the friction factor ratio to decline for all values of the radius ratio.
- The physics of flow mechanisms associated with various regimes were explored and discussed.

Finally, it is concluded that the results obtained from the present study are closer to those obtained by the researchers in the limiting sense and thus more reliable. These insights are particularly valuable for various industrial applications where fluid flow between rotating coaxial cylinders is critical. For instance, the results can be applied to the design and optimization of journal bearings, where the inner cylinder's rotation plays a pivotal role in maintaining lubrication and reducing friction. Similarly, in mixing equipment, understanding the flow characteristics of non-Newtonian fluids can improve mixing efficiency and product consistency, particularly in the food, pharmaceutical, and chemical industries. By extending the application of the Langlois Recursive Approach to these practical scenarios, this study not only advances theoretical understanding but also provides a robust foundation for solving real-world engineering challenges.

Furthermore, the study opens avenues for future research, including the exploration of transient flow behaviors, the impact of temperature variations. By extending the capabilities of LRA, more comprehensive models can be developed, leading to optimized designs and processes in various engineering fields.

## Author Contributions

F. Shaikh initiated and conceptualized the project and has prepared original draft; A. M.Siddqui reviewed original draft and critically analyzed and suggested; G.M. Memon worked on visualization; S. Feroz Shah technically reviewed and edited the manuscript. The manuscript was written through the contribution of all authors. All authors discussed the results, reviewed, and approved the final version of the manuscript.


## Acknowledgments

The authors acknowledge the Department of Basic Sciences and Related Studies, Mehran University of Engineering and Technology, Jamshoro 76090, Sindh, Pakistan, for providing a valuable and motivating research environment.


## Conflict of Interest

There is no conflict of interest.

## Funding

The authors received no financial support for the research, authorship, and publication of this article.


## Data Availability Statements

Not applicable.

## Nomenclature

| | | | |
|---|---|---|---|
| $\rho$ | Constant density (kgm$^{-3}$) | $\omega_1$ | Angular velocity of inner cylinder (rad.sec$^{-1}$) |
| $\eta$ | Zero shear viscosity (Pa.s) | $\beta$ | Pseudoplastic parameter |
| $V$ | Velocity vector of the fluid (m/s) | $\xi$ | Radius ratio |
| $V(r)$ | Velocity in tangential direction (m/s) | $R_i$ | Radius of inner cylinder (m) |
| $P$ | Pressure (Pa) | $R_o$ | Radius of outer cylinder (m) |
| $T$ | Stress tensor (Nm$^{-2}$) | | |
| $\varphi$ | Extra tensor (Nm$^{-2}$) | | |

## References


[1] Couette, M., Studies relating to the friction of liquids, *Annales de Chimie et de Physique*, 21(6), 1890, 433-510.

[2] Taylor, G. I., VIII. Stability of a viscous liquid contained between two rotating cylinders, *Philosophical Transactions of the Royal Society of London. Series A, Containing Papers of a Mathematical or Physical Character*, 223(605-615), 1923, 289-343.

[3] Giesekus, H., Zur stabilität von Strömungen viskoelastischer Flüssigkeiten: 1. Ebene und kreisförmige Couette-Strömung, *Rheologica Acta*, 5(3), 1966, 239-252.

[4] Tao, C., Kutchko, B. G., Rosenbaum, E., Massoudi, M., A review of rheological modeling of cement slurry in oil well applications, *Energies*, 13(3), 2020, 570.

[5] Elçiçek, H., Güzel, B., Effect of shear-thinning behavior on flow regimes in Taylor–Couette flows, *Journal of Non-Newtonian Fluid Mechanics*, 279, 2020, 104277.

[6] Kawaguchi, T., Tano, Y., Saito, T., Experimental studies on the Taylor-Couette flow of shear-thinning fluids, *GEOMATE Journal*, 23(97), 2022, 31-37.

[7] Reddy, Y. D., Mebarek-Oudina, F., Goud, B. S., Ismail, A. I., Radiation, velocity and thermal slips effect toward MHD boundary layer flow through heat and mass transport of Williamson nanofluid with porous medium, *Arabian Journal for Science and Engineering*, 47(12), 2022, 16355-16369.

[8] Abo-Dahab, S. M., Abdelhafez, M. A., Mebarek-Oudina, F., Bilal, S. M., MHD Casson nanofluid flow over nonlinearly heated porous medium in presence of extending surface effect with suction/injection, *Indian Journal of Physics*, 95(12), 2021, 2703-2717.

[9] Shaikh, K., Shaikh, F., Khokhar, R. B., Memon, K. N., Analytical Solution of Transient Flow of Fractional Oldroyd-B Fluid between Oscillating Cylinders, *VFAST Transactions on Mathematics*, 10(2), 2022, 21-33.

[10] Mebarek-Oudina, F., Chabani, I., Review on nano enhanced PCMs: insight on nePCM application in thermal management/storage systems, *Energies*, 16(3), 2023, 1066.

[11] Naseem, T., Mebarek-Oudina, F., Shahzad, A., Fish, H., Hamida, M. B., Enhanced thermodynamic irreversibility and heat transfer in rotating graphene oxide–water nanofluids over a stretching surface, *Modern Physics Letters B*, 40(03), 2026, 2550267.

[12] Aich, W., Abbas, T., Sewify, G. H., Sadiq, M. N., Khan, S. U., Bilal, M., Kolsi, L., Comparative numerical and analytical computations for magnetized pseudoplastic materialwith roll-coating applications, *Alexandria Engineering Journal*, 79, 2023, 538-544.

[13] Alam, M. K., Siddiqui, A. M., Rahim, M. T., Islam, S., Avital, E. J., Williams, J. J. R., Thin film flow of magnetohydrodynamic (MHD) pseudo-plastic fluid on vertical wall, *Applied Mathematics and Computation*, 245, 2014, 544-556.

[14] Mebarek-Oudina F., Convective heat transfer of Titania nanofluids of different base fluids in cylindrical annulus with discrete heat source, *Heat Transfer-Asian Research,* 48(1), 2019, 135-47.

[15] Mebarek-Oudina, F., Numerical modeling of the hydrodynamic stability in vertical annulus with heat source of different lengths, *Engineering Science and Technology, An International Journal*, 20(4), 2017, 1324-1333.

[16] Mebarek-Oudina, F., Aissa, A., Mahanthesh, B., Öztop, H. F., Heat transport of magnetized Newtonian nanoliquids in an annular space between porous vertical cylinders with discrete heat source, *International Communications in Heat and Mass Transfer*, 117, 2020, 104737.

[17] Daprà, I., Scarpi, G., Analytical solution for a Couette flow of a Giesekus fluid in a concentric annulus, *Journal of Non-Newtonian Fluid Mechanics*, 223, 2015, 221-227.

[18] Zeb, M., Islam, S., Siddiqui, A. M., Haroon, T., Homotopy Perturbation Method for Flow of a Third-grade Fluid Through a Vertical Concentric Annulus, *International Journal of Nonlinear Sciences and Numerical Simulation,* 13(3-4), 2012, 281-287.

[19] Memon, K. N., Mushtaque, A., Shaikh, F., Ghoto, A. A., Siddiqui, A. M., Delta Perturbation Method for Couette-Poiseuille flows in Third grade fluids, *VFAST Transactions on Mathematics*, 10(2), 2022, 1-12.

[20] Pantokratoras, A., Flow past a rotating sphere in a non-Newtonian, Carreau fluid, up to a Reynolds number of 1000, *Australian Journal of Mechanical Engineering*, 19(3), 2021, 317–327.

[21] Boger, D. V., Demonstration of upper and lower Newtonian fluid behaviour in a pseudoplastic fluid, *Nature*, 265(5590), 1977, 126-128.

[22] Deiber, J. A., Cruz, A., On Non-Newtonian Fluidflow Through a Tube of Circular Cross-Section, *American Journal of Chemical Engineering and Applied Chemistry,* 14(1), 1984, 19-38.

[23] Langlois, W. E., A recursive approach to the theory of slow, steadystate viscoelastic flow, *Transactions of the Society of Rheology*, 7(1), 1963, 75-99.

[24] Alibenyahia, B., Lemaitre, C., Nouar, C., Ait-Messaoudene, N., Revisiting the stability of circular Couette flow of shear-thinning fluids, *Journal of Non-Newtonian Fluid Mechanics*, 183, 2012, 37-51.

[25] Ravanchi, M. T., Mirzazadeh, M., Rashidi, F., Flow of Giesekus viscoelastic fluid in a concentric annulus with inner cylinder rotation, *International Journal of Heat and Fluid Flow*, 28(4), 2007, 838-845.

[26] Jouyandeh, M., M. Moayed Mohseni, Rashidi, F., Tangential flow analysis of giesekus model in concentric annulus with both cylinders rotation, *Journal of Applied Fluid Mechanics*, 10(6), 2017, 1721-1728.

[27] Raayai-Ardakani, S., McKinley, G. H., Geometry mediated friction reduction in Taylor-Couette flow, *Physical Review Fluids*, 5(12), 2020, 124102.



## ORCID iD

Fozia Shaikh https://orcid.org/0000-0002-1049-5268

Abdul Majeed Siddiqui https://orcid.org/0000-0001-9386-2387

Ghulam Mustafa Memon https://orcid.org/0000-0001-9339-1909

Syed Feroz Shah https://orcid.org/0000-0002-6964-1469

**How to cite this article:** Shaikh F., et al. Analytical Solution of the Flow of Pseudo-plastic Fluid with the Effect of Inner Rotating Cylinder, *J. Appl. Comput. Mech.*, xx(x), 2026, 1–13. https://doi.org/10.22055/jacm.2026.49355.5912